International Journal of Thermophysics, Vol. 20, No. 2, 1999

Solubilities, Vapor Pressures, and Heat Capacities of the Water + Lithium Bromide + Lithium Nitrate + Lithium Iodide + Lithium Chloride System

K.-K. Koo,[1,2] H.-R. Lee,[1] S. Jeong,[3] Y.-S. Oh,[4] D.-R. Park,[4] and Y.-S. Baek[4]

Received March 19, 1998

The optimum mole ratio of lithium salts in the $H_2O + LiBr + LiNO_3 + LiI + LiCl$ system was experimentally determined to be $LiBr : LiNO_3 : LiI : LiCl = 5 : 1 : 1 : 2$. The solubilities were measured at temperatures from 252.02 to 336.75 K. Regression equations on the solubility data were obtained with a least-squares method. Average absolute deviations of the calculated values from the experimental data were 0.15% at temperatures < 285.18 K and 0.05% at temperatures $\geqslant 285.18$ K. The vapor pressures were measured at concentrations ranging from 50.0 to 70.0 mass% and at temperatures from 330.13 to 434.88 K. The experimental data were correlated with an Antoine-type equation, and the average absolute deviation of the calculated values from the experimental data was 2.25%. The heat capacities were measured at concentrations from 50.0 to 65.0 mass% and temperatures from 298.15 to 328.15 K. The average absolute deviation of the values calculated by the regression equation from the experimental data was 0.24%.

KEY WORDS: absorption chiller; heat capacity; lithium bromide; lithium chloride; lithium iodide; lithium nitrate; solubility; vapor pressure.

1. INTRODUCTION

Currently, much attention is being paid to small-scale, air-cooled absorption chillers for residential use, because of increasingly stringent regulations

[1] Department of Chemical Engineering, Sogang University, C.P.O. Box 1142, Seoul 100-611, Korea.
[2] To whom correspondence should be addressed.
[3] Department of Mechanical Engineering, Sogang University, C.P.O Box 1142, Seoul 100-611, Korea.
[4] R&D Center, Korea Gas Corporation, Ansan 425-150, Korea.

0195-928X/99/0300-0589$16.00/0

against the use of chloroflorocarbon refrigerants and because of electric power shortage during summer time. In air-cooled systems, the operational temperature of the absorber is expected to be about 15°C higher than that of a water-cooled system, because of poor heat transfer characteristics of air. However, extension of the an absorption cycle with a conventional LiBr aqueous solution for an air-cooled system is often hampered by the crystallization of the working fluid. One way to resolve the crystallization problem is to modify LiBr-based aqueous solutions by adding organic and/or inorganic substances as anticrystallization agents. In order to examine the feasibility test of a new working fluid, extensive thermophysical properties including solubilities, vapor pressures, heat capacities, densities, viscosities, and surface tensions are required.

Many working pairs based on LiBr aqueous solutions have been considered recently. Physical and thermal properties, and corrosion characteristics of the $H_2O + LiBr + LiNO_3$ [1], $H_2O + LiBr + LiI$ [2–4], and $H_2O + LiBr + LiCl$ [5] systems have been reported in the literature. Here $LiNO_3$ behaves as an anticrystallization and anticorrosion agent. LiI is also selected as an anticrystallization agent, and LiCl acts as a vapor-pressure suppression agent. The $H_2O + LiBr + LiNO_3 + LiI + LiCl$ system was proposed as a potential working fluid for air-cooled absorption chillers [6]. However, experimental data on the thermophysical properties of this system have not been reported to date. Therefore, a systematic study has been undertaken to measure the thermophysical properties of this system.

In this communication, a procedure for determining the optimum mole ratio of the lithium salts from the solubility data of $H_2O + LiBr + LiNO_3$, $H_2O + LiBr + LiNO_3 + LiI$, and $H_2O + LiBr + LiNO_3 + LiI + LiCl$ systems is introduced. Secondly, for the $H_2O + LiBr + LiNO_3 + LiI + LiCl$ system with an optimum mole ratio, the most important properties for the theoretical analysis of refrigeration cycles, i.e., solubilities, vapor pressures, and heat capacities, are reported over a wide range of temperatures with correlation equations.

2. EXPERIMENTS

2.1. Materials

The LiBr (99 + %), LiI (99 + %), $LiNO_3$ (97 + %), and LiCl (99 + %) used in this work were supplied by Aldrich Chemical Co.. All reagents were used without further purification. All solutions were prepared using deionized distilled water.

2.2. Experimental Apparatus and Procedure

The solubility measurements were carried out with a visual polythermal method [7]. The main part of the solubility measurement system consists of an equilibrium cell and a thermostat (Lauda, RM20S) stabilized to within ± 0.01 K. The cell is a 100-ml Pyrex glass vessel with a triple jacket. The inner side of the cell contains the salt solution. The heating medium from the thermostat is circulated through the middle layer of the cell. The outer jacket of the cell was hermetically sealed under vacuum to prevent fogging on the surface of the cell during experiments at lower temperatures and allows us to observe easily the formation or melting of crystals. This configuration is also effective for keeping the temperature constant by preventing heat loss from the wall.

The sample solution of about 30 ml in the cell is cooled to crystallize at a rate of $1\ \mathrm{K} \cdot \mathrm{min}^{-1}$. First, a rough estimation of the crystallization temperature is made. Then the sample solution is heated with a controlled heating rate as the crystals are melted. When a few crystals remain, the heating rate is controlled to be $0.003\ \mathrm{K} \cdot \mathrm{min}^{-1}$. At this heating rate, the melting point of the last crystal of salt is taken to be the equilibrium saturation temperature. At a temperature 10 K higher than the equilibrium saturation temperature, the solution is kept for about 1 h to ensure that all remaining crystals are dissolved. Then the solution is cooled again. As the temperature of the solution approaches the expected crystallization temperature, the cooling rate is controlled to $0.1\ \mathrm{K} \cdot \mathrm{min}^{-1}$. Finally, the crystallization temperature is determined when the first crystal forms.

The vapor pressure was determined using a boiling-point method [8, 9]. The experimental setup consists of a 500-ml round-bottom flask as an equilibrium still, a condenser, a mercury manometer, and a vacuum pump. The equilibrium still with the sample solution (about 250 ml) is placed in the thermostat equipped with a cooler and heater. With this assembly the thermostat was found to be stable within ± 0.01 K during the experimental runs.

The sample solution in the still with a magnetic bar is placed in the thermostat. The thermostat is maintained at room temperature. Coolant is supplied to the condenser by another thermostat (Lauda, RM20S) with a temperature of 0°C. When the temperature of the solution and the thermostat reaches equilibrium, the system is evacuated to about 10^{-4} Torr. The vapor pressure is determined with a manometer at the equilibrium temperature between the still and the thermostat.

The heat capacities were measured using an isoperibol solution calorimeter (Calorimetry Sci. Co., Model 4300). The calorimeter consists of a 25-ml Dewar vessel, an electric heater for temperature equilibrium and

calibration, a thermistor, a glass stirrer, and a thermostat. All measuring procedures were completely controlled by a computer. The heat capacities of the sample solution were calculated with Eq. (1) using the temperature difference calculated by the computer.

$$Q = (mC_p + \varepsilon)\,\Delta T \tag{1}$$

where Q is the total heat added, m is the sample mass, C_p is the heat capacity ($kJ \cdot kg^{-1} \cdot K^{-1}$) of the sample, and ε is the heat capacity ($kJ \cdot K^{-1}$) of the apparatus including the Dewar vessel, stirring rod, heater, and thermistor. The value of ε was calculated by the experimental results using water as the standard.

3. RESULTS AND DISCUSSION

3.1. Determination of Optimum Mol Ratio of Salts

Figure 1 shows the crystallization temperatures of the $H_2O + LiBr + LiNO_3$ system with 58.0, 60.0, and 62.5 mass% lithium salts. As the mole ratio of $LiBr/LiNO_3$ increases, the crystallization temperatures were found to decrease and to reach a minimum. Then the crystallization temperatures were found to increase slowly as the $LiBr/LiNO_3$ ratio increases. As can be seen from Fig. 1, crystallization temperatures of the proposed system, compared with those of the $H_2O + LiBr$ system given by Boryta [10], were

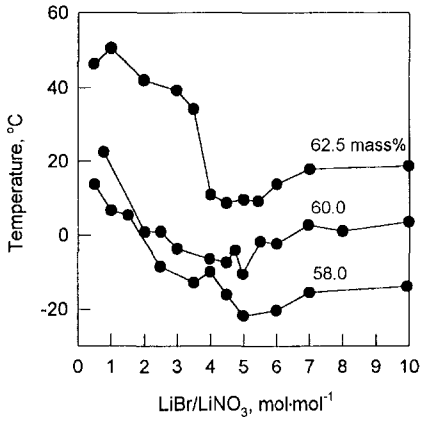

Fig. 1. Crystallization temperatures of the $H_2O + LiBr + LiNO_3$ system with the mole ratio of $LiBr/LiNO_3$.

found to drop about 15 to 20 K in the present experimental range. As can be seen from the figure, the optimum mole ratio is clearly shown to be about 5 in the $H_2O + LiBr + LiNO_3$ system.

The optimum mole ratio of $LiBr : LiNO_3 : LiI$ in the $H_2O + LiBr + LiNO_3 + LiI$ system was determined by a procedure similar to that for the $H_2O + LiBr + LiNO_3$ system. Figure 2 illustrates the variation of the crystallization temperature with the $LiI/LiNO_3$ ratio in the $H_2O + LiBr + LiNO_3 + LiI$ system in which the mole ratio of LiBr to $LiNO_3$ is fixed to be 5. In that figure, at solution concentrations of 60.0 and 62.5 mass%, the optimum mole ratio of $LiI/LiNO_3$ is shown to be about 1. The crystallization temperature of the $H_2O + LiBr + LiNO_3 + LiI$ system was found to decrease further, about 30 to 35 K lower than that of the $H_2O + LiBr$ system. However, the vapor pressure of this four-component system was much higher than that for the $H_2O + LiBr$ system as shown in Fig. 3. To suppress the vapor pressure, LiCl was added. The vapor suppression effect of LiCl was found to be satisfactory as can be seen from Fig. 3. When the mole ratio of LiCl was 2.0 to 2.5, the vapor pressure of the proposed system was found to be close to that of the $H_2O + LiBr$ system. However, when the LiCl/LiI ratio is over 2.0, it was found that the addition of LiCl adversely affects the solubility enhancement (not shown here). From these experimental observations, the optimum mole ratio of $LiBr : LiNO_3 : LiI : LiCl$ was determined to be 5 : 1 : 1 : 2 at a concentration of 60.0 mass% lithium salts in the $H_2O + LiBr + LiNO_3 + LiI + LiCl$ system.

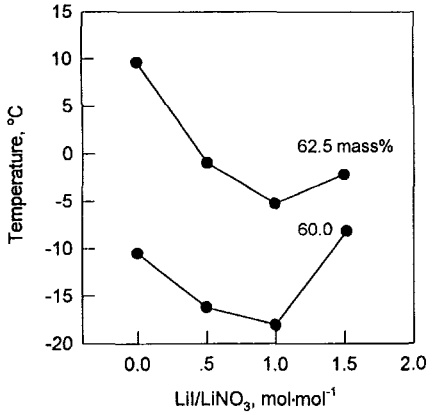

Fig. 2. Effect of LiI on the solubility of the $H_2O + LiBr + LiNO_3 + LiI$ system ($LiBr/LiNO_3 = 5$, by mol).

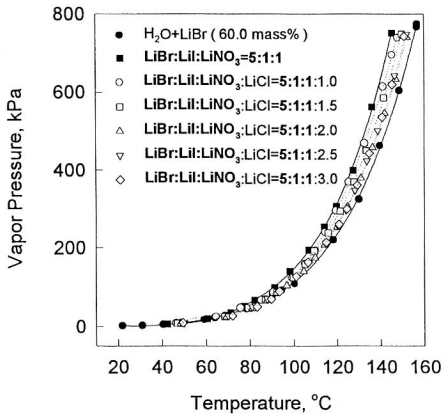

Fig. 3. Vapor pressures of the $H_2O + LiBr + LiNO_3 + LiI + LiCl$ system (concentration: 60.0 mass%).

3.2. Solubility

The solubilities for the system ($LiBr : LiNO_3 : LiI : LiCl = 5 : 1 : 1 : 2$, by mol) were measured with a visual polythermal method at temperatures from 252.02 to 336.75 K. The measured mass fractions are listed in Table I. The experimental data for the solution have been fitted to the following equation by a least-squares method:

$$S = \sum_{i=0}^{2} A_i T^i \tag{2}$$

where S is the solubility in mass percentage of absorbent (lithium salts), T is the absolute temperature, and A_i are the coefficients. The values of the coefficients are listed in Table II. In Fig. 4, experimental data are compared with values calculated from the fitted equation and with those of the $H_2O + LiBr$ system [10]. This figure clearly demonstrates that the solubility is enhanced in the entire temperature range of the experiments. The average absolute deviation between experimental and calculated values is 0.15% when the solution temperature is below 285.18 K and 0.05% when the solution temperature is above 285.18 K.

3.3. Vapor Pressure

The vapor pressures of the $H_2O + LiBr + LiNO_3 + LiI + LiCl$ system ($LiBr : LiNO_3 : LiI : LiCl = 5 : 1 : 1 : 2$, by mol) were measured at concentrations

Table I. Solubilities of the $H_2O + LiBr + LiNO_3 + LiI + LiCl$ System ($LiBr : LiNO_3 : LiI : LiCl = 5 : 1 : 1 : 2$, by mol)

Temperature (K)	Concentration (mass%)
252.02	60.0
271.29	61.5
277.06	62.5
281.07	63.3
282.24	64.0
284.10	64.5
285.18	64.8
286.91	65.0
299.54	65.9
311.89	67.0
319.81	67.9
336.75	69.4

Table II. Calculated Values of the Coefficients in Eq. (2)

A_i	$T < 285.18$ K	$T \geq 285.18$ K
A_0	3.95339×10^{2}	6.14451×10^{1}
A_1	-2.63307×10^{0}	-5.41117×10^{-2}
A_2	5.16831×10^{-3}	2.21139×10^{-4}

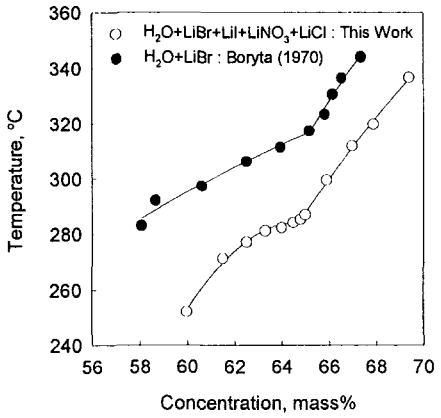

Fig. 4. Solubilities of the $H_2O + LiBr + LiNO_3 + LiI + LiCl$ system ($LiBr : LiNO_3 : LiI : LiCl = 5 : 1 : 1 : 2$, by mol).

from 50.0 to 70.0 mass% and temperatures from 330.13 to 434.88 K. The experimental results are listed in Table III and are plotted in Fig. 5 against the reciprocal of temperature. As can be seen in Fig. 5, a $\log P$ vs $1000/(T-43.15)$ relation for the given concentrations was linear over the pressure and temperature ranges. The vapor pressures were correlated with an Antoine-type equation which expresses vapor pressure as a function of temperature and concentration as follows:

$$\log P = \sum_{i=0}^{4} [A_i + \{1000B_i/(T-43.15)\}](100X)^i \tag{3}$$

Table III. Vaport Pressures of the $H_2O + LiBr + LiNO_3 + LiI + LiCl$ System ($LiBr : LiNO_3 : LiCl = 5 : 1 : 1 : 2$, by mol)

Temp. (K)	Pressure (kPa)	Temp. (K)	Pressure (kPa)	Temp. (K)	Pressure (kPa)	Temp. (K)	Pressure (kPa)
50.0 mass%		51.8 mass%		55.0 mass%		58.0 mass%	
330.13	4.21	342.71	7.13	334.21	3.81	32.36	2.75
338.54	6.78	353.53	12.24	345.16	6.42	361.84	11.00
350.71	12.35	360.78	16.94	367.54	19.11	369.37	16.02
360.54	19.45	368.13	24.91	376.18	28.28	374.70	20.36
369.44	28.02	375.37	33.32	384.73	40.12	383.05	29.12
377.93	39.68	382.16	43.08	394.12	54.27	390.54	38.86
386.47	54.78	394.10	64.17			399.04	52.09
394.12	70.78	400.66	81.51			404.83	65.51
401.43	90.19	408.09	99.44				
405.01	98.92						
60.0 mass%		62.5 mass%		65.0 mass%		70.0 mass%	
354.40	6.15	362.34	7.13	370.17	7.61	383.37	9.47
361.06	8.77	384.94	19.83	375.43	10.02	394.92	15.73
370.08	13.85	394.37	28.62	383.85	14.51	409.05	26.93
377.93	18.78	403.71	40.24	401.38	29.15	421.30	41.33
383.18	23.35	411.82	54.29	407.95	39.15		
387.59	27.66	419.52	71.99	415.20	51.35		
393.21	33.78	430.68	99.37	422.49	64.05		
398.13	40.93			427.75	77.15		
404.26	50.61			434.88	99.19		
409.72	61.08						
415.18	72.67						
420.26	84.42						
425.53	98.64						

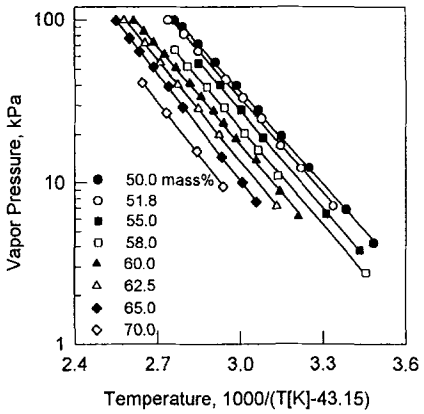

Fig. 5. Vapor pressures of the $H_2O + LiBr + LiNO_3 + LiI + LiCl$ system ($LiBr : LiNO_3 : LiI : LiCl = 5 : 1 : 1 : 2$, by mol).

where P is the vapor pressure in kPa, T is the absolute temperature, and X is the mass fraction of salts. The coefficients A_i and B_i have been determined by a least-squares method and are listed in Table IV. The average absolute deviation of lathe calculated values from the experimental data was 2.25%.

3.4. Heat Capacity

The heat capacities of the $H_2O + LiBr + LiNO_3 + LiI + LiCl$ system ($LiBr : LiNO_3 : LiI : LiCl = 5 : 1 : 1 : 2$, by mol) were measured at concentrations from 50.0 to 65.0 mass% and temperatures from 298.15 to 328.15 K.

Table IV. Calculated Values of the Coefficients in Eq. (3)

A_i	Value	B_i	Value
A_0	-1.276429×10^3	B_0	4.374120×10^2
A_1	8.764646×10^1	B_1	-3.008232×10^1
A_2	-2.233375×10^0	B_2	7.690697×10^{-1}
A_3	2.517102×10^{-2}	B_3	-8.697553×10^{-3}
A_4	-1.058556×10^{-4}	B_4	3.669313×10^{-5}

Table V. Heat Capacities of the $H_2O + LiBr + LiNO_3 + LiI + LiCl$ System ($LiBr : LiNO_3 : LiI : LiCl = 5 : 1 : 1 : 2$, by mol)

Temperature (K)	C_p(kJ · kg^{-1} · K^{-1})			
	50.0 mass%	55.0 mass%	60.0 mass%	65.0 mass%
298.15	2.250	2.126	2.006	1.912
303.15	—	—	—	1.914
308.15	2.260	2.140	2.022	1.918
313.15	—	—	—	1.924
318.15	2.250	2.138	2.027	1.912
323.15	—	—		1.927
328.15	2.268	2.152	2.025	1.927

Table VI. Calculated Values of the Coefficients in Eq. (4)

Ai	Value	B_i	Value	C_i	Value
A_0	-2.173879×10^{3}	B_0	1.402895×10^{1}	C_0	-2.261076×10^{-2}
A_1	1.189572×10^{2}	B_1	-7.661341×10^{-1}	C_1	1.234024×10^{-3}
A_2	-2.150578×10^{0}	B_2	1.383909×10^{-2}	C_2	-2.227713×10^{-5}
A_3	1.285306×10^{-2}	B_3	-8.266132×10^{-5}	C_3	1.329870×10^{-7}

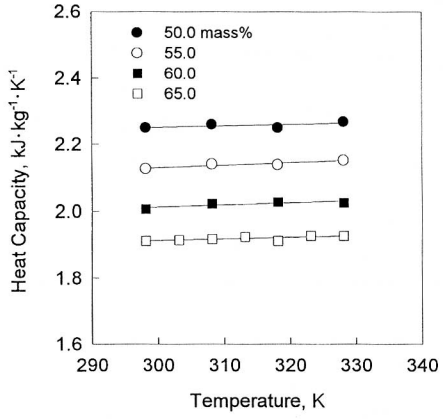

Fig. 6. Heat capacities of the $H_2O + LiBr + LiNO_3 + LiI + LiCl$ system ($LiBr : LiNO_3 : LiI : LiCl = 5 : 1 : 1 : 2$, by mol).

The experimental results are listed in Table V and were fitted to the following equation:

$$C_p = \sum_{i=0}^{3} [A_i + B_i T + C_i T^2](100X)^i \tag{4}$$

where C_p is the heat capacity ($kJ \cdot kg^{-1} \cdot K^{-1}$), A_i, B_i, and C_i are the regression parameters, T is the absolute temperature, and X is the mass fraction of the lithium salts. The parameters A_i, B_i, and C_i were determined by a least-squares method and are listed in Table VI. The average absolute deviation between the experimental and the calculated values was 0.24%. The experimental and calculated results of heat capacity measurements are plotted in Fig. 6. This figure indicates that the heat capacity of the solution increased slightly with temperature.

4. CONCLUSIONS

The solubilities, the vapor pressures, and the heat capacities of the $H_2O + LiBr + LiNO_3 + LiI + LiCl$ system were measured at various temperatures and concentrations. The optimum mole ratio of the lithium salts was determined by solubility measurements of the $H_2O + LiBr + LiNO_3$, the $H_2O + LiBr + LiNO_3 + LiI$, and the $H_2O + LiBr + LiNO_3 + LiI + LiCl$ systems and the ratio of $LiBr : LiNO_3 : LiI$ LiCl was found to be 5 : 1 : 1 : 2. The proper correlation equations were obtained from the experimental results of solubilities, vapor pressures, and heat capacities. The values calculated from the equations were found to be in good agreement with the experimental data. The solubility and vapor pressure data suggest that the proposed five-component system has the potential to be a working fluid for air-cooled absorption machines. All the experimental data reported in the present work can be used to construct the Dühring and enthalpy–concentration diagrams for the theoretical analysis of refrigeration cycles.

REFERENCES

1. S. Iyoki, R. Yamanaka, and T. Uemura, *Int. J. Refrig.* **16**:191 (1993).
2. S. Iyoki, S. Iwasaki, Y. Kuriyama, and T. Uemura, *J. Chem. Eng. Data* **38**:302 (1993).
3. S. Iyoki, S. Iwasaki, Y. Kuriyama, and T. Uemura, *J. Chem. Eng. Data* **38**:396 (1993).
4. S. Iyoki, S. Iwasaki, and T. Uemura, *J. Chem. Eng. Data* **35**:429 (1990).
5. T. Uemura, *Refrigeration* **68**:699 (1993).

6. T. Okino, Y. Asawa, M. Fusimoto, N. Nishiyama, and Y. Sanai, *AES-Vol. 3, International Absorption Heat Pump Conference* (ASME, 1993), p. 311.
7. M. A. Clynee and R. W. Potter II, *J. Chem. Eng. Data* **24**:338 (1979).
8. G. Scatchard, C. L. Raymond, and H. H. Gilmann, *J. Am. Chem. Soc.* **60**:1275 (1938).
9. G. Scatchard, S. E. Wood, and J. M. Mochel, *J. Am. Chem. Soc.* **62**:712 (1940).
10. D. A. Boryta, *J. Chem. Eng. Data* **15**:142 (1970).